Conserved interdomain linker promotes phase separation of the multivalent adaptor protein Nck

Sudeep Banjade[a,b], Qiong Wu[a], Anuradha Mittal[c], William B. Peeples[a,b], Rohit V. Pappu[c], and Michael K. Rosen[a,b,1]

[a]Department of Biophysics, UT Southwestern Medical Center, Dallas, TX 75390; [b]Howard Hughes Medical Institute, UT Southwestern Medical Center, Dallas, TX 75390; and [c]Department of Biomedical Engineering and Center for Biological Systems Engineering, Washington University in St. Louis, St. Louis, MO 63130

Edited by Barry Honig, Howard Hughes Medical Institute, Columbia University, New York, NY, and approved August 19, 2015 (received for review May 5, 2015)

The organization of membranes, the cytosol, and the nucleus of eukaryotic cells can be controlled through phase separation of lipids, proteins, and nucleic acids. Collective interactions of multivalent molecules mediated by modular binding domains can induce gelation and phase separation in several cytosolic and membrane-associated systems. The adaptor protein Nck has three SRC-homology 3 (SH3) domains that bind multiple proline-rich segments in the actin regulatory protein neuronal Wiskott-Aldrich syndrome protein (N-WASP) and an SH2 domain that binds to multiple phosphotyrosine sites in the adhesion protein nephrin, leading to phase separation. Here, we show that the 50-residue linker between the first two SH3 domains of Nck enhances phase separation of Nck/N-WASP/nephrin assemblies. Two linear motifs within this element, as well as its overall positively charged character, are important for this effect. The linker increases the driving force for self-assembly of Nck, likely through weak interactions with the second SH3 domain, and this effect appears to promote phase separation. The linker sequence is highly conserved, suggesting that the sequence determinants of the driving forces for phase separation may be generally important to Nck functions. Our studies demonstrate that linker regions between modular domains can contribute to the driving forces for self-assembly and phase separation of multivalent proteins.

phase separation | multivalency | interdomain linker | adaptor proteins | intrinsically disordered

Eukaryotic cells are compartmentalized into different organelles, which have specific functions. Membrane-bound organelles, such as the endoplasmic reticulum and vacuoles, have been studied extensively, and their functions are relatively well understood. Non–membrane-bound organelles also exist in cells. These organelles include P-granules, Cajal bodies, promyelocytic leukemia (PML) bodies, paraspeckles, and the nucleolus, for example (1). Recently, many of these non–membrane-bound structures have been proposed to form via liquid–liquid demixing phase transitions of their constituent molecules (protein, DNA, and RNA) (2). For example, germ-line P-granules and the nucleolus show liquid-like properties, including droplet fusion, fission, and shearing, and they dissolve and condense in a fashion reminiscent of a phase separation process (3–5). Similarly, stress granules also condense and dissolve, sequestering the family of DYRK kinases (6). Organelles, such as the centrosome, have also been studied through the lens of phase separation (7).

A molecular understanding of the physical properties that promote formation of new phases is important for understanding the nature, function, and regulation of non–membrane-bound organelles. We recently showed that multivalent proteins interact with multivalent ligands to form higher order species in aqueous solution that phase-separate and give rise to liquid droplets. The constituent proteins are highly concentrated in these droplets (~100-fold) (8). This phenomenon appears to be general for multivalent proteins; we have observed it for both natural and engineered systems involving both protein–protein and protein–RNA interactions (8). When one of the interacting species is tethered to a membrane, multivalent polymerization and phase separation can also result in formation of analogous dynamic puncta on the surface of the membrane (9). A recent study demonstrated a similar multivalency-based behavior based on constituents of the mRNA decapping machinery (10). In that work, interactions between high-valency helical Leu-like motifs and the oligomeric RNA-binding protein LSm caused the formation of a separate liquid phase.

These studies have emphasized the formation of large oligomers through the interactions of ordered domains. These domains bind their ligands through well-defined molecular interfaces, with affinities in the range of 1–100 μM through specific interactions to form discrete complexes. The connection of the domains by flexible tethers has been regarded largely as a mechanism to achieve multivalency and promote dynamics in the ligand-induced 3D networks. In other studies, however, disordered regions of proteins, particularly those regions composed of low-complexity amino acid sequences, have been found to promote phase separation in vitro and in cells (11–15) and to promote association with RNA granules (11, 12, 16, 17). These disordered elements can self-associate, leading to liquid droplets (15) or hydrogels (11, 12), with the former being apparently isotropic and latter being enriched in amyloid-like fibers. These studies highlight the importance of disordered regions in the molecular self-assembly leading to formation of phase-separated structures in cells.

The adaptor protein Nck and its orthologs function in signaling pathways that control diverse cellular processes, including axon guidance, cell movement, cell–cell fusion, stress responses, and maintenance of cell–cell adhesions (18–23). In many cases, these responses are coupled to the polymerization of actin through

Significance

Many eukaryotic proteins are composed of tandem arrays of modular domains, which bind peptide ligands that also often appear in tandem arrays. The interdomain linkers in such systems are often considered merely passive elements that flexibly connect the functional domains. Collective interactions among multivalent molecules lead to micron-sized phase-separated states that are thought to be important in cellular organization. Here, we show that in the multivalent signaling adaptor protein Nck, weak interactions involving an interdomain linker play a significant role in self-assembly and phase separation with ligands neuronal Wiskott-Aldrich syndrome protein (N-WASP) and phosphorylated nephrin. Our results suggest that interactions mediated by ordered modular domains may generally act synergistically with weak interactions of disordered interdomain linkers to promote phase separation.

Author contributions: S.B., R.V.P., and M.K.R. designed research; S.B., Q.W., A.M., and W.B.P. performed research; S.B., Q.W., A.M., W.B.P., R.V.P., and M.K.R. analyzed data; and S.B., R.V.P., and M.K.R. wrote the paper.

The authors declare no conflict of interest.

This article is a PNAS Direct Submission.

[1]To whom correspondence should be addressed. Email: michael.rosen@utsouthwestern.edu.

This article contains supporting information online at www.pnas.org/lookup/suppl/doi:10.1073/pnas.1508778112/-/DCSupplemental.

Nck/neuronal Wiskott-Aldrich syndrome protein (N-WASP)/Arp2/3 complex pathways (24–29). Nck is composed of an SRC homology 2 (SH2) domain and three SRC-homology 3 (SH3) domains; the former binds phosphotyrosine (pTyr) in pYDEV sequence motifs, and the latter bind a variety of proline-rich motifs (PRMs) (14, 30, 31). These modules are connected by linkers ranging from 24 to 50 residues that are predicted based on amino acid sequence to be intrinsically disordered (32, 33). NMR analysis of Nck2 has shown that the linkers are mostly disordered, although a portion of the linker between the first and second SH3 domains interacts weakly with the latter domain (32). We have demonstrated that Nck phase-separates upon interaction with PRMs in its ligand, N-WASP, and that this process occurs at lower concentrations in the presence of the pTyr-containing ligand, phosphorylated nephrin (p-nephrin) (8, 9). Phase separation is dependent upon the number of pTyr motifs in p-nephrin and SH3 domains in Nck.

Other than the NMR study cited above, the possible functions of linkers in Nck have, to the best of our knowledge, not been systematically examined. The linkers are often viewed as passive, flexible tethers between the SH2 and SH3 domains. In this study, we demonstrate that the linker between the first and second SH3 domains of Nck can affect the phase separation behavior of p-nephrin/Nck/N-WASP oligomers. The linker consists of a basic N-terminal element and an acidic C-terminal element. The basic element promotes phase separation of Nck assemblies through two short linear motifs, as well as its overall positively charged character. This effect correlates with increased self-assembly of Nck, which NMR analyses and computer simulations suggest may be mediated by weak interactions of the linear motifs with the second SH3 domain. Taken together with analysis of the linker-mediated phase behavior, our data suggest that weak interactions of the linker act synergistically with higher affinity interactions of the modular domains (SH3-PRM and SH2-pTyr) to promote collective interactions among the constituent molecules that give rise to phase separation. Given that the sequence compositions and lengths of the linkers in different adaptor proteins are highly variable, these disordered regions may help specify when and where phase separation occurs in biological multivalent systems.

Results

Linker Between the First and Second SH3 Domains Can Promote Phase Separation of Nck Constructs. The three SH3 domains of Nck share 27–30% pairwise amino acid sequence identity to each other. Previous studies have suggested that the different domains have different binding specificities for PRMs (31, 34–36). To eliminate these differences and isolate valency as the examined parameter, our recent investigation of p-nephrin/Nck/N-WASP on supported bilayers used engineered Nck-like proteins containing tandem repeats of the second Nck SH3 domain. This work demonstrated that phase separation is dependent on both the number of SH3 domains in Nck and the number of pTyr sites in p-nephrin, supporting the idea that phase separation is driven by collective interactions of multivalent species (9) (Fig. 1*A*).

Here, we began by asking if differences between the three SH3 domains in natural Nck might add complexity to this simple model. To test for specific roles of the different SH3 domains, we engineered a series of Nck truncation mutants containing only two SH3 domains (plus the SH2 domain) and examined their ability to phase-separate in the presence of N-WASP (plus 7.5 μM triple p-nephrin in all phase separation experiments hereafter, except where explicitly noted). We term the SH3 domains of Nck S1, S2, and S3, from N-terminal to C-terminal. We term the linkers between these domains L1 and L2, respectively, and we term the linker between S3 and the SH2 domain L3 (Fig. 1*B*).

We varied the concentration of an N-WASP fragment containing the basic, proline-rich, and VCA (verprolin homology,

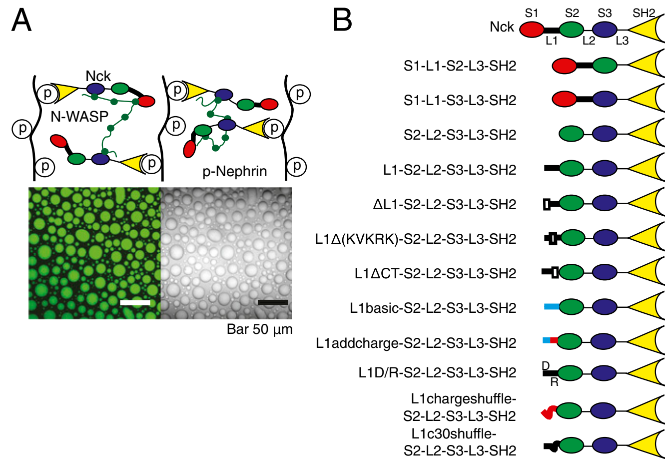

Fig. 1. Multivalent interactions in adaptor proteins drive phase separation. (*A*, *Top*) Model of the interaction of the multivalent proteins p-nephrin, Nck, and N-WASP. (*A*, *Bottom*) Upon mixing 3 μM p-nephrin, 2 μM N-WASP (10% Alexa488-labeled), and 10 μM Nck, micrometer-scale droplets can be visualized by fluorescence (*Left*) and differential interference contrast (*Right*) microscopies. (*B*) Some constructs based on Nck used in this study.

central and acidic) regions of the protein (named simply N-WASP hereafter) and the various Nck proteins. Varying full-length Nck and N-WASP in concert (i.e., moving along the diagonal of the phase diagram), phase separation is observed at 5 μM of both proteins (8) (Fig. 2*A* and *SI Appendix*, Fig. S1; note that in the complete phase diagram, phase separation is observed with as little as 5 μM Nck and 1 μM N-WASP). With the divalent molecules S1-L1-S2-L3-SH2 and S1-L1-S3-L3-SH2, phase separation is observed at a concentration of 20 μM plus 20 μM N-WASP (Fig. 2 *B* and *C*). The increase in the concentration required for phase separation with loss of S3 or S2, respectively, is consistent with the valency dependence observed previously with the engineered Nck-like proteins (9). Further, the data suggest that S2 and S3 make similar contributions to phase separation, because exchanging them produces identical behavior. However, to our surprise, the divalent molecule S2-L2-S3-L3-SH2 does not phase-separate even up to a concentration of 250 μM plus 250 μM N-WASP (Fig. 2*D*). Thus, the three divalent molecules are not equivalent in their ability to drive phase separation.

To examine whether different binding specificities of the SH3 domains could account for these observations, we measured the affinities of each domain for a panel of PRM peptides derived from N-WASP by NMR spectroscopy. We analyzed 12 peptides consisting of individual PRMs, as well as three peptides consisting of two PRMs (Table 1). In each case, we titrated unlabeled peptide into ^{15}N-labeled SH3 domain and fit the ^{1}H and ^{15}N chemical shifts of the domain, measured in $^{1}H/^{15}N$ heteronuclear single quantum coherence (HSQC) spectra, to a single-affinity binding isotherm. The dissociation constants (K_ds) for the binding of S1 to the individual PRMs ranged from 255 to 1,080 μM, with some values too weak to measure (K_d > 1,080 μM); the diPRM constructs had apparent K_d values greater than or equal to 720 μM, suggesting negative cooperativity compared with some of the individual PRM peptides (Table 1). S2 had dissociation constants ≥150 μM against the single PRMs and ≥64 μM for the diPRMs (Table 1). S3 had behavior similar to S2, with K_d values against individual PRMs ≥220 μM and against diPRMs ≥67 μM. In general, S2 and S3 had similar patterns of affinities for the various peptides and typically bound with higher affinity than did S1. The similar affinity patterns of S2 and S3 toward the PRMs are also consistent with the identical phase separation behaviors of

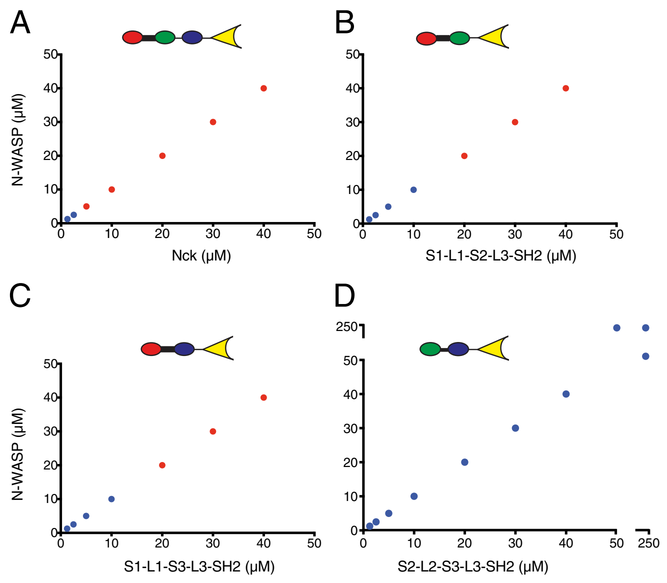

Fig. 2. Different di-SH3 fragments of Nck are not equivalent in their phase separation properties. Phase separation of N-WASP and Nck proteins in the presence of 7.5 μM p-nephrin is shown. Red and blue symbols indicate phase separation and no phase separation, respectively. (*A*–*D*) Data for Nck, S1-L1-S2-L3-SH2, S1-L1-S3-L3-SH2, and S2-L2-S3-L3-SH2, respectively.

S1-L1-S2-L3-SH2 and S1-L1-S3-L3-SH2. However, the binding affinities appear insufficient to explain the absence of phase separation by S2-L2-S3-L3-SH2, because S2 and S3 bind better than S1 to virtually every peptide, and thus should promote oligomerization more strongly.

Another difference between constructs that phase-separate and constructs that do not was the presence and absence of L1, which was previously shown to bind to S2 in an autoinhibitory fashion (32) (Fig. 2). Therefore, we added the L1 motif to the inactive divalent construct to produce L1-S2-L2-S3-L3-SH2. This construct phase separated at a concentration of 30 μM plus 30 μM N-WASP (Figs. 3 *A* and *B*). Thus, L1 was able to impart the ability to phase-separate to an apparently inactive di-SH3 protein. An L1-only peptide does not phase-separate at concentrations as high as 2 mM, suggesting that the effect of the linker is synergistic with multivalent interactions of the SH3 domains of Nck with the PRMs of N-WASP.

Positively Charged Element in L1 Promotes Phase Separation. The sequence of L1 shows a striking distribution of charges, with a highly basic N terminus and a highly acidic C terminus (Fig. 3*A*). All but one of its 10 basic residues lie within its N-terminal half, and all but one of its six acidic residues lie within its C-terminal half. This distribution is conserved across evolution from fish to humans, and also in Nck2.

To understand how L1 promotes phase separation, we initially examined several L1-S2-L2-S3-L3-SH2 constructs lacking different portions of the linker. A construct lacking the first 17 residues of the N-terminal basic region (ΔL1-S2-L2-S3-L3-SH2) did not phase-separate up to 250 μM concentration plus 250 μM N-WASP (Fig. 3*C*). Mutation of three Lys residues in this region to Glu (L1K/E-S2-L2-S3-L3-SH2) or deletion of the central KVKRK motif (L1ΔKVKRK-S2-L2-S3-L3-SH2), which was previously shown to interact with S2 (32), had similarly deleterious effects on phase separation (Fig. 3 *D* and *E*, respectively). However, replacing the C-terminal 25 amino acids with an uncharged $(GGSA)_3$ linker did not affect phase separation, producing liquid droplets at a concentration of 30 μM plus 30 μM N-WASP (L1ΔCT-S2-L2-S3-L3-SH2; Fig. 3*F*). Thus, in the context of the di-SH3 proteins, two regions of L1 appear to be most important for promoting phase separation: the 17 N-terminal residues and the central KVKRK motif.

In systems composed of disordered regions with linear binding motifs, the amino acid sequence contexts of those motifs (i.e., the flanking regions) can influence their interactions with ligands. Because basic elements within the N terminus are important for phase separation, we asked whether the degree of positive charge in L1 could affect phase separation (*SI Appendix*, Fig. S2*A*). Increasing the overall positive charge in L1 (L1basic; *SI Appendix*, Fig. S2*B*) or increasing the positive charge density in the N-terminal element (L1addcharge and L1D/R) enhances the driving force for phase separation such that phase separation is observed at concentrations of 10 or 20 μM di-SH3 protein plus 10 or 20 μM N-WASP (*SI Appendix*, Fig. S2 *C* and *D*, respectively). In contrast, shuffling charged residues throughout L1 (L1charge-shuffle) or all residues in the C-terminal 30 amino acids (L1c30shuffle) leads to impairment of phase separation (*SI Appendix*, Fig. S2 *E* and *F*, respectively). It is noteworthy that both sets of mutations also perturb the central KVKRK motif. The combined mutagenesis data suggest a model in which two regions, the N-terminal 17 residues and the KVKRK motif, as well as the overall positive charge/positive charge density in the sequence, are responsible for the promotion of phase separation by L1.

We also observed similar effects of L1 perturbations in full-length Nck. In experiments performed in the presence of 7.5 μM

Table 1. Affinities of the individual Nck SH3 domains for PRMs in N-WASP

PRM	Sequence	SH3-1 K_d, μM	SH3-2 K_d, μM	SH3-3 K_d, μM
1	LRRQAPPPPPPS	>1 mM	235 ± 16	231 ± 36
2	APPPPPPSRGG	>1 mM	348 ± 24	289 ± 42
3	RGGPPPPPPPPH	420 ± 22.1	N.B.	1,650 ± 115
4	GPPPPPARGRGA	>1 mM	147 ± 4	222 ± 29
5	ARGRGAGAPPPPPS	N.B.	295 ± 23	527 ± 84
6	GAPPPPPSRAPT	1,080 ± 94	288 ± 23	∼800
7	TAAPPPPPPSRP	>1 mM	701 ± 70	N.B.
8	VAVPPPPPNRMY	255 ± 20.7	199 ± 8	∼1 mM
9	NRMYPPPPPALP	700	N.B.	>>1 mM
10	SAPSGPPPPPPSVL	>1 mM	N.B.	>>1 mM
11	VAPPPPPPPPPPPG	346 ± 24.1	N.B.	>>1 mM
12	PGPPPPPGLPSD	N.B.	N.B.	>>1 mM
diPRM-1	LRRQAPPPPPPSRGGPPPPPPPPH	720 ± 97	88 ± 38	114 ± 28
diPRM-2	GPPPPPARGRGAPPPPPSRAP	∼1,500	64 ± 8	67 ± 6
diPRM-3	VPPPPPNRMYPPPPPALPS	∼900	160 ± 19	∼1 mM

N.B., no binding.

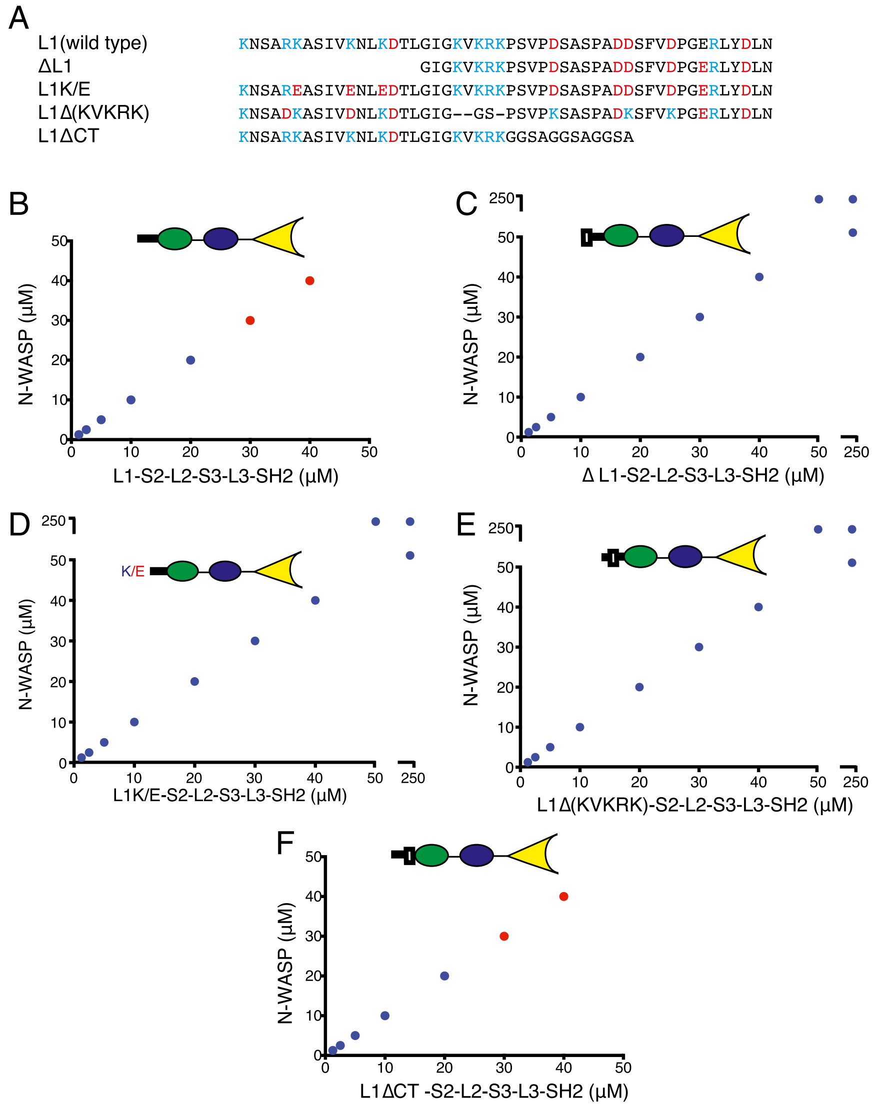

Fig. 3. L1 promotes phase separation of a di-SH3 protein through a basic N-terminal element. (*A*) Sequences of L1 used in experiments shown in *B*–*G*. (*B*–*G*) Phase separation experiments were performed in the presence of 7.5 μM p-nephrin. Red and blue symbols indicate phase separation and no phase separation, respectively.

p-nephrin, Nck (WT) induces phase separation at a concentration of 5 μM plus 5 μM N-WASP (*SI Appendix*, Fig. S3*B*). A construct where L1 is replaced with a (Gly-Gly-Ser-Ala)$_{10}$ linker [Nck(L1ggsa)] requires a concentration of 40 μM plus 40 μM N-WASP to phase-separate (*SI Appendix*, Fig. S3*C*). Deletion of 15 residues from the N terminus of L1 (Nck ΔL1b) shifts the phase separation boundary to a concentration of 20 μM plus 20 μM N-WASP (*SI Appendix*, Fig. S3*D*), as does shuffling the entire L1 sequence (Nck L1shuffle; *SI Appendix*, Fig. S3*E*). Therefore, the enhancement of phase separation by L1 occurs consistently across a wide range of di-SH3 and full-length Nck proteins, and appears to depend on the degree and density of positive charge in the sequence. We note that because Nck has higher SH3 valency than the di-SH3 proteins, polymer theory predicts that its propensity to oligomerize (and thus phase-separate) should be less affected by the added valency provided by L1 interactions, consistent with our data (37). A summary of the constructs examined here and their phase separation behaviors is presented in *SI Appendix*, Fig. S4.

L1 Promotes Self-Assembly of Nck. We focus the remainder of our analysis on the mechanism by which L1 promotes phase separation. We used isothermal titration calorimetry to compare the affinity of L1-S2-L2-S3-L3-SH2 and L1chargeshuffle-S2-L2-S3-L3-SH2 for N-WASP. Although this experiment is complicated by the presence of multiple SH3 domains and multiple PRMs in the respective partners, a simple 1:1 model of the binding isotherms yielded essentially identical apparent K_d values of 54 μM and 58 μM for L1-S2-L2-S3-L3-SH2 and L1chargeshuffle-S2-L2-S3-L3-SH2, respectively (Fig. 4*A*). These affinities are not higher than the affinities of the individual SH3 domains for the di-PRM peptides (Table 1). Together, the calorimetry and NMR data suggest that L1 does not substantially increase the affinity of the di-SH3 proteins for N-WASP. L1 did not substantially decrease the affinity either, as might be expected based on the work of Takeuchi et al. (32), likely because of the very low affinity of the L1–S2 interaction (discussed below). Thus, the difference in phase separation behavior of these constructs is probably not due to differential ability to bind N-WASP. Further, as shown in *SI Appendix*, Fig. S5 *A* and *B*, the ability of L1 to promote phase separation does not require p-nephrin, suggesting that the effect is not due to increased affinity of the Nck SH2 domain for pTyr

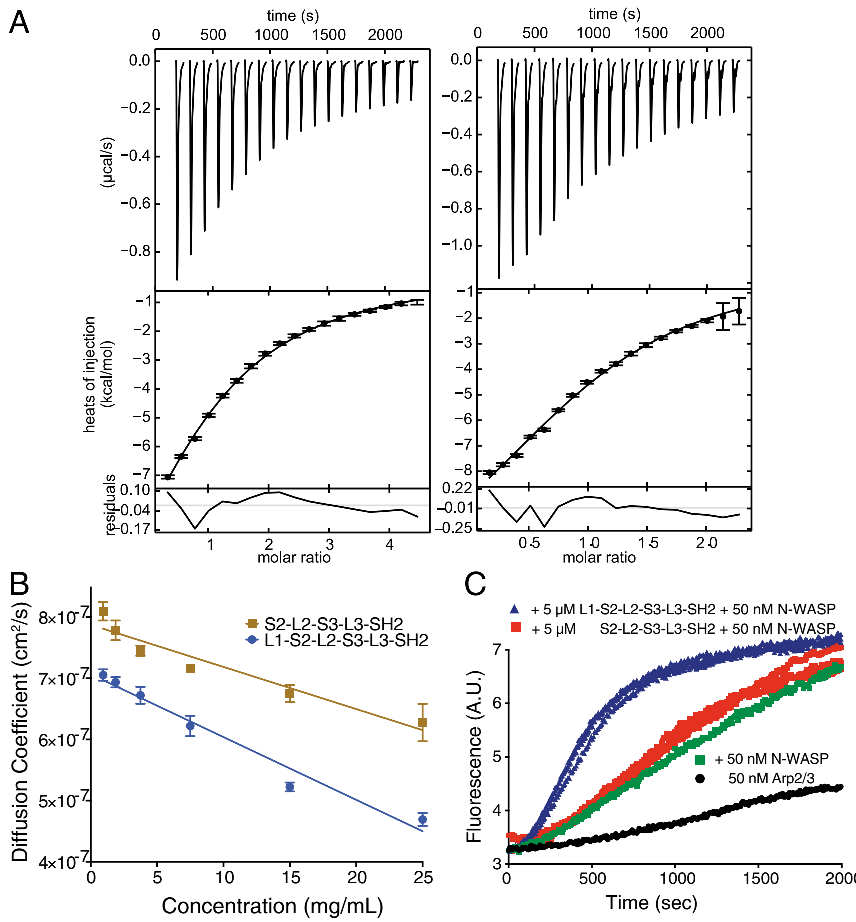

Fig. 4. L1 promotes self-association of di-SH3 proteins but does not substantially alter binding to N-WASP. (*A*) Isothermal titration calorimetry analysis of the binding of L1-S2-L2-S3-L3-SH2 or L1chargeshuffle-S2-L2-S3-L3-SH2 to N-WASP. A total of 1.1 mM of L1-S2-L2-S3-L3-SH2 was titrated to 100 μM N-WASP (*Left*) and 1.1 mM L1chargeshuffle-S2-L2-S3-L3-SH2 was titrated to 50 μM N-WASP (*Right*), thereby giving different molar ratios in the *x* axis. Heats of injection (*Upper*), single-site fit to integrated heats (*Middle*), and residuals of the fit (*Lower*), respectively, are shown. (*B*) Diffusion coefficients of L1-S2-L2-S3-L3-SH2 (brown squares) and S2-L2-S3-L3-SH2 (blue circles) at different concentrations, measured by DLS. Error bars indicate replicates from three different protein preparations. (*C*) Pyrene-actin assembly assays contained 2 μM actin (5% pyrene-labeled) and 50 nM Arp2/3 complex (black), plus 50 nM N-WASP (green), 50 nM N-WASP and 5 μM S2-L2-S3-L3-SH2 (red), or 50 nM N-WASP and 5 μM L1-S2-L2-S3-L3-SH2. Data for S2-L2-S3-L3-SH2 and L1-S2-L2-S3-L3-SH2 reflect three replicates.

motifs. Thus, L1 does not appear to act by enhancing modular SH3-PRM or SH2-pTyr interactions.

We next asked whether L1 might promote self-association of Nck. We used dynamic light scattering (DLS) to measure the diffusion coefficients of the di-SH3 proteins as a function of concentration (Fig. 4*B*). The construct containing L1 (L1-S2-L2-S2-L3-SH2) showed decreasing diffusion coefficients as the concentration increased from 1 to 25 mg/mL (27.6 to 690.9 μM). Over this same concentration range, the construct lacking L1 (S2-L2-S2-L3-SH2) showed a smaller decrease. These data indicate that the Nck constructs can weakly self-associate, and that L1 enhances this effect. As described below, NMR data support a similar conclusion (Fig. 5).

To assess self-association mediated by electrostatic interactions involving L1 further, we examined the salt dependence of the DLS data. We measured the diffusion coefficients of diSH3 proteins containing either WT L1 or L1chargeshuffle in buffer containing 150–750 mM KCl (*SI Appendix*, Fig. S5*C*). At lower KCl concentrations (150 mM and 250 mM), the L1-S2-L2-S3-L3-SH2 protein shows lower diffusion coefficients than the L1chargeshuffle-S2-L2-S3-L3-SH2 protein, suggesting greater self-association in the WT L1 protein. The diffusion coefficient of the WT construct increases significantly as salt concentration is raised, consistent with disruption of intermolecular electrostatic interactions. At KCl concentrations higher than 500 mM, the diffusion coefficient of the WT construct equals the diffusion coefficient of the charge-shuffled mutant, which is less sensitive to salt than the WT. The combined data suggest that L1 has a propensity to enhance Nck self-association due to electrostatic interactions. These interactions are weakened either by the screening in high salt or by the screening that is encoded by shuffling the charge, thus weakening the linear charge density. We note that the concentrations used in the DLS experiments are appreciably higher than the concentrations required for phase separation, indicating that the enhancement of association due to L1 is very weak. Nevertheless, when acting in concert with multivalent SH3–PRM interactions, such weak effects are evidently significant.

We previously showed that dimerization or, more generally, oligomerization of N-WASP increases activity toward the Arp2/3 complex, due to the presence of two binding sites for the N-WASP VCA region on the Arp2/3 complex (38, 39). We asked if the weak self-association of L1 in the presence of multivalent SH3–PRM interactions could also increase the activity of N-WASP in Arp2/3-mediated pyrene-actin assembly assays (40) (Fig. 4*C*). In such assays, the fluorescence of pyrene-labeled actin increases upon incorporation of the protein into filaments such that changes

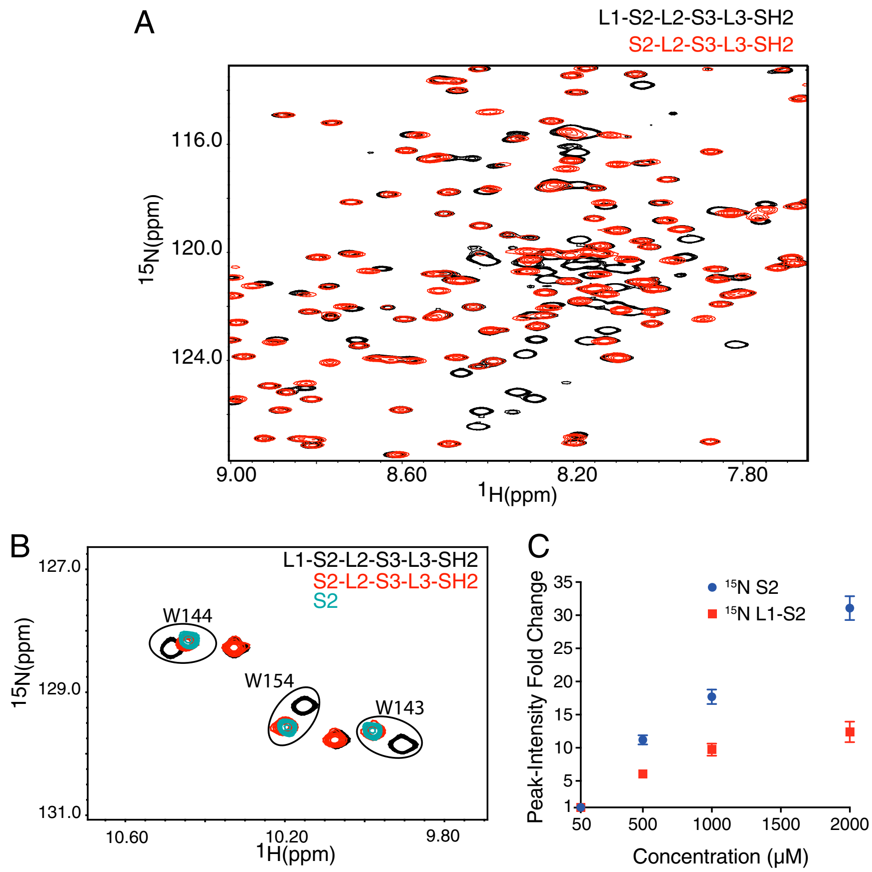

Fig. 5. L1 is partially disordered, and also binds the second SH3 domain. (*A*) Overlaid $^1H/^{15}N$ TROSY spectra of 250 μM U-[^{15}N] labeled L1-S2-L2-S3-L3-SH2 (black) and 250 μM S2-L2-S3-L3-SH2 (red). (*B*) Overlaid Trp indole region of $^1H/^{15}N$ TROSY spectra of L1-S2-L2-S3-L3-SH2 (black), 250 μM S2-L2-S3-L3-SH2 (red), and 310 μM S2 (blue). (*C*) Average fold change (±SD) in intensities of 15 peaks from S2 in $^1H/^{15}N$ HSQC spectra of ^{15}N-labeled L1-S2 and S2 at the indicated concentrations. Intensities were normalized to the intensities at 50 μM.

in fluorescence report on the kinetics of filament formation. Addition of 5 μM S2-L2-S3-L3-SH2 to assays containing 50 nM N-WASP, 50 nM Arp2/3 complex, and 2 μM actin (5% pyrene-labeled) had no effect on the kinetics of actin assembly. However, addition of 5 μM L1-S2-L2-S3-L3-SH2 decreased the lag time and increased the rate of assembly, indicating higher N-WASP activity (Fig. 4*C*). These experiments were performed without nephrin, in conditions where phase separation does not occur. Furthermore, the construct we use does not include the GTPase binding domain (GBD) region of N-WASP; therefore, the increase in activity toward the Arp2/3 complex is not due to regulation of autoinhibition of N-WASP (41). These data are consistent with the idea that L1 enhances the self-association of Nck/N-WASP complexes.

Overall, the correlation between stronger self-association and the promotion of phase separation among the di-SH3 constructs examined here (S2-L2-S3-L3-SH2 ~ L1chargeshuffle-S2-L2-S3-L3-SH2 < L1-S2-L2-S3-L3-SH2) suggests that these properties are related. Thus, weak self-association of Nck through positively charged elements in L1 could act cooperatively with stronger SH3–PRM and SH2–pTyr interactions to promote phase separation in the p-nephrin/Nck/N-WASP system.

The effect of enhancement in phase separation by L1 also occurs, although to a lesser degree, in an independent system of multivalent proteins. A protein consisting of five small ubiquitin-like modifier (SUMO) domains fused to five SUMO interaction motifs (SIMs) through a $(GGS)_4$ linker ($SUMO_5$-SIM_5; *SI Appendix*, Fig. S5*D*) phase-separates at 12 μM. However, a protein in which $SUMO_5$ and SIM_5 are connected by L1 ($SUMO_5$-L1-SIM_5) phase-separates at 4 μM. A protein in which L1 is replaced with L1chargeshuffle phase separates at 10 μM, quite similar to the construct containing a $(GGS)_4$ linker ($SUMO_5$-L1chargeshuffle-SIM_5; *SI Appendix*, Fig. S5*D*). Thus, the effects of L1 are not entirely specific to the p-nephrin/Nck/N-WASP system. Rather, the linker can act autonomously to promote the phase separation of multivalent proteins. This observation suggests that the charged blocks of residues can interact nonspecifically with charges on the surfaces of other protein partners, but when the acidic and basic residues are shuffled to decrease the local charge density, these interactions are diminished. In this regard, it is probably important that like S2 and S3 of Nck, both $SUMO_5$ and SIM_5 are acidic (pI = 5.34 and 4.07, respectively) and that SUMO structures show a prominent acidic surface patch, which could enable favorable interactions with the basic element of L1. In the context of multivalent binding, these weak interactions could produce an enhancement in assembly of these complexes.

L1 Can Interact with the Second SH3 Domain of Nck. To learn how L1 might promote self-assembly of Nck, we examined $^1H/^{15}N$ transverse relaxation-optimized spectroscopy (TROSY) spectra of several ^{15}N-labeled Nck proteins. The spectrum of L1-S2-L2-S3-L3-SH2 shows a large number of well-dispersed resonances, indicative of folded domains, as well as a series of intense, poorly dispersed resonances, representing disordered, dynamic residues (Fig. 5*A* and *SI Appendix*, Fig. S6*A*). Deletion of L1, which eliminates 48 backbone amides of the protein, causes the disappearance of 36 resonances, all of which are in the poorly dispersed region (^1H chemical shifts between 7.8 and 8.7 ppm). The disparity between the total number of residues and the number of resonances lost suggests that 12 residues in L1 are undergoing chemical exchange, and thus have highly broadened/missing resonances in the L1-S2-L2-S3-L3-SH2 spectrum. In addition to eliminating many cross-peaks, loss of L1 causes shifts in 18 backbone cross-peaks of lower intensity, 15 of which are in the well-dispersed regions of the spectrum (^{1}H chemical shifts <7.8 ppm and >8.7 ppm) (*SI Appendix*, Fig. S6*A*). Three Trp side-chain cross-peaks shift as well (Fig. 5*B*). Overlaying the spectrum of isolated S2 reveals that all of these shifting cross-peaks correspond to this domain (Fig. 5*B* and *SI Appendix*, Fig. S6*A*). Thus, our data suggest that as in Nck2, L1 of Nck contacts S2.

To understand this interaction better, we further analyzed the spectra of L1-S2 and S2 constructs, which could be assigned with greater completeness and certainty than the spectra of the longer proteins. Consistent with data on the longer proteins, resonances from L1 in the L1-S2 protein show poor chemical shift dispersion. Furthermore, peaks corresponding to the C-terminal acidic portion of L1 have high and relatively uniform intensity, whereas peaks in the N terminus are appreciably weaker (*SI Appendix*, Fig. S6*B*). Five of the N-terminal 11 residues could not be assigned due to exchange broadening; the first Lys residue of the KVKRK motif also could not be assigned. Notably, these regions correspond well to the elements of L1 that promote phase separation (Fig. 3).

As in the longer proteins, loss of L1 also causes substantial changes in chemical shift to 18 backbone amide resonances in S2 (*SI Appendix*, Fig. S7*A*) and all three Trp indole cross-peaks. Mapping these crosspeaks to the S2 structure shows that they localize to one face of the domain (*SI Appendix*, Fig. S7*B*), with highest density near one end of the canonical PRM binding site (*SI Appendix*, Fig. S7*B*, denoted by a circle). Notably, the highly acidic Arg–Thr loop (RT loop) is located near the center of the affected region, and all five of its residues are perturbed (E120-R121-E122-D123-E124; *SI Appendix*, Figs. S6 and S7). This site overlaps with the L1 binding site in Nck2 previously identified by Takeuchi et al. (32).

Interestingly, comparing ^{1}H/^{15}N HSQC spectra of S3 and an engineered L1–S3 fusion showed chemical shift changes of many residues belonging to S3 upon deletion of L1 (*SI Appendix*, Fig. S8*A*), suggesting that L1 can also make *cis*-interactions with S3 when fused directly to it. This effect likely explains the ability of the S1-L1-S3-L2-SH2 construct to phase-separate (Fig. 2*C*). We note that S2 and S3 are both acidic (pI = 4.6), suggesting that the basic nature of L1 could allow it to interact with acidic ordered domains in proximity.

We also used atomistic simulations based on the ABSINTH implicit solvation model and force-field paradigm (42) to obtain atomic-level insights regarding the pattern and likelihoods of contacts that might form between L1 and S2. The construct for these simulations was Ac-L1-S2-Nme, where Ac and Nme, respectively, refer to *N*-acetyl and *N*′-methylamide capping groups. For the simulations, we used the recently developed Hamiltonian switch-metropolis Monte Carlo (HS-MMC) methodology that is designed to enhance conformational sampling of disordered regions tethered to ordered domains (43). The details of the simulation methodology and the analysis are presented in *SI Appendix*. The main results are summarized in *SI Appendix*, Figs. S9 and S10. *SI Appendix*, Fig. S9*A* shows the ensemble-averaged interresidue distances we compute within L1 and between L1 and S2. We performed 10 independent HS-MMC runs, and the patterns of contacts are consistent across all 10 runs. *SI Appendix*, Figs. S9*B* and S10 provide quantitative summaries of the probabilities associated with observing persistent interresidue contacts between the L1 and S2 domains. The results point to a pattern of interdomain distances that is suggestive of spatial proximity between residues within the N-terminal half of L1 and the acidic surface of S2, specifically the RT loop and residues in its spatial neighborhood. The simulation results are in accord with the NMR experiments and suggest that spatially proximal contacts between the N-terminal half of L1 and the S2 domain (smallest distances ≤3.5 Å) are observed in 2–5% of the conformations sampled. In addition, the simulated ensembles show a consistent pattern of intermediate-range distances being sampled between the residues of the N-terminal half of L1 and the acidic surface of S2. A representative conformation demonstrating the types of interdomain contacts that can form is shown in *SI Appendix*, Fig. S9*C*.

Finally, we also examined intermolecular binding of L1 to S2. First, we recorded ^{1}H/^{15}N HSQC spectra of S2 in the presence of various concentrations of an isolated L1 protein (*SI Appendix*, Fig. S8 *B* and *C*). Addition of L1 causes progressive changes in many resonances of S2. The pattern of affected resonances is very similar to the pattern observed in comparing the S2 and L1-S2 spectra, indicating that the interaction occurs in similar fashion *in trans* and *in cis* (*SI Appendix*, Fig. S7 *A* and *B*). Fitting the chemical shift changes *in trans* to a single-site binding isotherm yields a K_d value of ∼1.3 mM, similar to the K_d value previously measured by Takeuchi et al. (32) for Nck2 (∼1.7 mM). We further examined intermolecular binding of L1 by measuring the intensity of peaks in ^{1}H/^{15}N HSQC spectra of S2 and L1-S2 as a function of concentration between 50 μM and 2,000 μM (Fig. 5*C*). As expected for a noninteracting system, intensities of S2 peaks scale nearly linearly with concentration. In contrast, peak intensities for L1-S2 are highly nonlinear with concentration due to line-broadening. Together, these data suggest that at higher concentrations, binding of L1 to S2 *in trans* can cause self-assembly of the protein through interactions analogous to those interactions occurring *in cis* at lower concentrations.

The simplest explanation for our NMR and simulation data are that in L1-S2-L2-S3-L3-SH2 (and, by inference, full-length Nck itself), residues within the N-terminal half of L1 that include the KVKRK motif make low-likelihood contacts with the surface of the S2 in a region that is spatially proximal to the acidic RT loop, in or near the PRM binding site. At low concentrations, these interactions are predominantly *in cis*. However, they can also occur *in trans* at high concentrations. In the context of p-nephrin/Nck/N-WASP assemblies, where multiple Nck proteins are held in close proximity, the weak interactions likely promote Nck self-assembly and, consequently, phase separation. We recognize that if L1 interacts with the PRM binding site, this interaction could increase the apparent valency of Nck (by enabling multiple molecules to come together), but at the expense of total free SH3 concentration in solution. Nevertheless, the interaction of L1 *in trans* would increase the sizes of the complexes formed, decreasing their solubility (37) and therefore promoting phase separation.

Discussion

Phase separation of biological molecules into distinct liquid-like structures may be a general approach used by cells to form and regulate non–membrane-bound compartments. We previously demonstrated that phase transitions can result from collective interchain interactions between multivalent proteins and their multivalent ligands (8). The collective effects of multiple specific interactions between modular elements (with K_ds in the 1–100 μM range for the binding of pairs of modules) can lead to increased local concentration of complementary modules and the formation of a system-spanning network (i.e., a sol-gel transition). Our observations are in accord with theories that have been developed to describe the phase behavior of linear chains that have multiple complementary binding modules and are also characterized by weak, nonspecific self-associations (44). According to these theories, multivalent polymers with complementary binding modules can undergo phase transitions through a combination of demixing driven by weak nonspecific self-associations and a sol-gel transition that is realized through collective interactions among networks of binding modules.

Linkers between binding modules are necessary for generating multivalent proteins with complementary binding modules. These linkers need not just be passive generators of multivalency. They can also serve as scaffolds for linear interaction motifs. Additionally, they can drive self-associations or compete for complementary interactions with ordered domains. We used the behavior of Nck and its ligands p-nephrin and N-WASP to examine the interplay between modular domain interactions and the properties of interdomain linkers. We have found that the linker between the first and second SH3 domains of Nck can promote phase separation of multivalent assemblies with N-WASP and p-nephrin. This effect is seen for both di-SH3 and tri-SH3 Nck constructs, and in complexes with N-WASP alone and those complexes containing all three proteins. This property of the linker results from three sequence features, namely, the N-terminal 17 residues, the central KVKRK motif, and the basic character of the N-terminal half of the sequence. For several constructs, the enhancement of phase separation correlates with an increased ability to promote weak Nck self-association, but not with higher affinity Nck/N-WASP or Nck/p-nephrin binding. Thus, increased self-association of Nck may be the mechanism by which the linker promotes phase separation of Nck/N-WASP and p-nephrin/Nck/N-WASP complexes. NMR analyses and atomistic simulations provide a potential "structural" mechanism for self-association, by revealing weak specific interactions of L1 to the second SH3 domain of Nck. The correspondence of the sequence motifs in L1 that bind the SH3 domain (*SI Appendix*, Fig. S6) with those sequence motifs that promote phase separation (Fig. 3 and *SI Appendix*, Figs. S2–S4), as well as the acidic character of the interaction site on the SH3 domain (*SI Appendix*, Fig. S7C) and the importance of the overall basic character of L1 in promoting phase separation (*SI Appendix*, Fig. S2), support the idea that L1–SH3 interactions provide the mechanism for L1 to promote phase separation. At high concentrations, this interaction can also occur *in trans*, which enables self-binding. We note that L1 also enhances phase separation in the S1-L1-S3-SH2 and polySUMO-polySIM systems, which obviously lack the second Nck SH3 domain. Nevertheless, both proteins are characterized by acidic surfaces (S3, SUMO, and SIM). We found that L1 can bind to S3 (*SI Appendix*, Fig. 8A), and we speculate that the acidic regions of SUMO and/or SIM could similarly bind weakly to the basic element of L1, leading to self-assembly and phase separation.

ClustalW analysis of ~50 Nck sequences reveals that the protein is highly conserved from fish to mammals, with average pairwise identity to human Nck1 of ~95% across the entire sequence. The average pairwise identity in the linker (94.9%; Fig. 6) is comparable to the average pairwise identity in the three SH3 domains (95.1%, 95.7%, and 94.8%, respectively) and the SH2 domain (97.3%), and slightly higher than the average pairwise identity in L2 and L3 (89.5% and 86.3%, respectively). The strong conservation of the linkers is unusual for multidomain proteins, suggesting that the properties of these elements in Nck are functionally important, perhaps through a general role of self-assembly and phase separation in Nck pathways. In this regard, it is notable that a large number of reported Nck ligands have three or more predicted or demonstrated pTyr binding sites for the Nck SH2 domain (45, 46), which would enable them to promote polymerization and phase separation analogous to p-nephrin.

Proteomic analysis has shown that several Ser and Thr residues in the basic region of L1 can be phosphorylated in cells (47, 48). The importance of the basic N-terminal region in the behavior of L1 suggests that these phosphorylation events could be used to regulate the phase separation of Nck assemblies, because the phosphorylation of the N-terminal residues would likely be inhibitory toward self-association of Nck. To our knowledge, Nck phosphorylation has not yet been examined in the context of localization/assembly or biological function of the protein. Such analyses will be needed to test these potential regulatory mechanisms in the future.

In addition to promoting phase separation of Nck constructs, we observed that L1 can enhance actin assembly through the Arp2/3 complex. We previously demonstrated that the affinity of N-WASP for the Arp2/3 complex is increased ~100-fold by dimerization. This effect suggests that the activity of assemblies containing autoinhibited N-WASP should increase with their size, due to the increased probability of containing two active conformers (38). Our actin assembly data here are consistent with low-level oligomerization of N-WASP (below the phase separation concentration) through the linker–SH3 interaction. We previously demonstrated that phase-separated droplets have much higher activity in Arp2/3-mediated actin assembly assays (8). This activity likely arises because the droplets contain large polymers of N-WASP. We hypothesize that in cells, low-level association of N-WASP would have modest effects on activation of the Arp2/3 complex, whereas phase separation would act in a switch-like fashion to enhance activity greatly.

Our investigations here have all used an N-WASP construct that lacks the GBD of the protein. In native N-WASP, the GBD binds a helix from the VCA element in an intramolecular fashion, blocking interactions of the latter with the Arp2/3 complex. This autoinhibition can be relieved by the Cdc42 GTPase, which destabilizes the GBD, releasing the VCA (49, 50). The accompanying paper by Okrut et al.

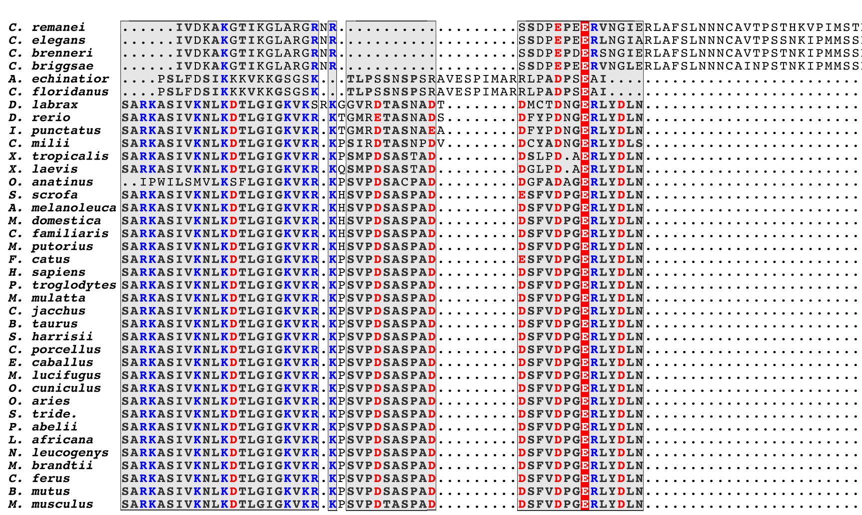

Fig. 6. L1 is highly conserved. Sequence alignment of the L1 region in Nck1 generated by ESPript (58). Conserved charged residues are colored blue for basic residues and red for acidic residues.

(51) reports that the L1 region of Nck can also bind the GBD of N-WASP, leading to activation toward the Arp2/3 complex. In this context, the N-terminal basic region of L1 forms a helix that appears to displace the VCA by structural mimicry. Interestingly, the EspFu protein from the pathogen enterohaemorrhagic *Escherichia coli* (EHEC) which hijacks the N-WASP/Arp2/3 pathway during infection, uses an identical mechanism to drive N-WASP activation (52). The L1–GBD interaction would provide an additional mechanism of cross-linking in Nck/N-WASP assemblies. In native systems, this interaction likely acts together with the L1–S2 interaction that we have described here to promote oligomerization (and potentially phase separation) of these molecules. The relative contributions of the two L1 binding modes could be regulated by Cdc42, whose binding should block the L1–GBD interaction by destabilizing the GBD. The consequences of such switching of L1 interactions on oligomerization, phase separation, and signaling to the Arp2/3 complex remain to be explored.

Even a cursory analysis of the interdomain linkers of different adaptor proteins demonstrates wide variability in lengths and sequence compositions. Our findings here suggest that adaptors containing linkers with blocks of charges may be more prone to phase separation than those adaptors with more evenly distributed charges. Interactions between opposite charges could occur between linkers and ordered domains, between two different linkers, or even between charged surfaces of ordered elements. The nature of the linkers is expected to influence the propensity to phase-separate, along with features such as module-module binding affinity, avidity effects, and module valency (8), and could provide additional mechanisms of regulation. Fine-tuning of these properties likely specifies which multivalent molecules are capable of forming supramolecular polymers and phase-separating in vivo. Biophysical and computational studies, based on these ideas, may be helpful in identifying molecules and pathways that could function and be regulated through phase separation.

Materials and Methods

Protein Expression and Purification. Extended protein purification and information on the constructs used are included in *SI Appendix*, *Materials and Methods*. Briefly, all proteins were expressed in BL21(DE3)T1R. Constructs of Nck and its mutants were expressed as a GST-fused protein. The proteins were purified by affinity purification using glutathione Sepharose beads (GE Healthcare), cleaved with tobacco etch virus (TEV) protease to remove the GST tag, and then applied through ion exchange and size-exclusion chromatography columns. Nephrin was expressed with an N-terminal maltose binding protein tag and a TEV protease site, as well as a C-terminal His6 tag preceded by a Prescission protease site, and was affinity-purified using nickel-nitrilotriacetic acid (Ni-NTA) agarose beads (Qiagen); the tags were cleaved using TEV and Prescission proteases, and the nephrin was then applied through ion exchange and size-exclusion purification methods. Purified protein was phosphorylated using the Lck kinase. His6 N-WASP (basic, proline-rich, and VCA regions) was purified using Ni-NTA agarose, the His6 tag was cleaved using a TEV protease, and the purified His6 N-WASP was then applied through ion exchange and size-exclusion chromatography columns.

Phase Separation Assays. Corning 384-well plates (catalog no. 3712) were washed with Milli-Q (Millipore) water and then with ethanol, and they were then dried under argon. Plates were then incubated with 0.1% BSA in 150 KMEI buffer [150 KCl, 1 mM $MgCl_2$, 1 mM EGTA, 10 mM imidazole (pH 7), and 1 mM DTT] for 10 min, and the BSA was washed twice with 100 μL of 150 KMEI buffer. Proteins were mixed at the indicated concentrations in 150 KMEI buffer. Droplet formation was visualized after 2 h of incubation at room temperature using a bright-field microscope.

Dynamic Light Scattering. Proteins were centrifuged at 16,000 × g for 10 min before analyses. Scattering experiments were performed at 22 °C using a DynaPro DLS instrument from Wyatt. Fifty runs of 20-s acquisition times were averaged to calculate the diffusion coefficient at each concentration. Intensities that deviated by >5% were excluded from the analyses.

Peptide Synthesis. PRM peptides were synthesized at the UT Southwestern proteomics center. To facilitate absorbance measurements and concentration determination, Trp was added at the N terminus of the peptides.

Actin Assembly Assays. Actin assembly experiments were performed as described earlier (40) using a high-throughput multiwell plate fluorimeter from Varioskan. The experiments were performed in 150 KMEI buffer. The concentrations of Arp2/3 complex and actin used were 50 nM and 2 μM, respectively. Fifty nanomolar N-WASP (B-P-VCA regions) was used in the presence of 5 μM L1-S2-L2-S3-L3-SH2 or S2-L2-S3-L3-SH2.

Isothermal Titration Calorimetry. Proteins were dialyzed in the same buffer [150 KMEI and 1 mM Tris(2-carboxyethyl)phosphine (TCEP) in the same vessel] before using them for isothermal calorimetry measurements. Measurements were performed at 15 °C on an iTC200 instrument from GE Healthcare. Isotherms were analyzed using the software NITPIC (53), and fits were performed using the software SEDPHAT (54).

NMR Spectroscopy. $^1H/^{15}N$ HSQC or $^1H/^{15}N$ TROSY experiments were performed with ^{15}N-labeled L1, L1-S2-L2-S3-L3-S3, S2-L2-S3-L3-S3, and S2 proteins on Varian 500 (600-MHz or 800-MHz) spectrometers at 25 °C. In the K_d measurements, the initial concentration of the SH3 domains was 100 μM. PRM peptides were titrated from concentrated aqueous stock solutions into the SH3 domains. Spectra were processed using NMRPipe (55) and NMRView (56). Dissociation constants were derived from fits to single-site binding isotherms.

Peaks that appear in the $^1H/^{15}N$ HSQC spectrum of L1-S2-L2-S3-L3-SH2 but not in the $^1H/^{15}N$ HSQC spectrum of S2-L2-S3-L3-SH2 were assumed to be in L1 and were assigned using HNCaCb, CbCa(CO)NNH, and CCC-TOCSY-NNH experiments (57). L1-S2 and S2 were fully assigned through the same experiments. Chemical shift perturbation (CSP) values in *SI Appendix*, Fig. S7A were determined according to:

$$\mathrm{CSP} = \sqrt{(\Delta\delta HN)^2 + (\Delta\delta N)^2 / 25}$$

where $\Delta\delta HN$ and $\Delta\delta N$ equal the difference in amide ^1H and amide ^{15}N chemical shifts, respectively, between S2 and either L1-S2 (for *in cis* CSP) or S2 + 2.5 mM L1 peptide (for *in trans* CSP).

ACKNOWLEDGMENTS. We thank Thomas Scheuermann and Chad Brautigam at the UT Southwestern Molecular Biophysics Resource for assistance with isothermal titration calorimetry; Haydn Ball at UT Southwestern proteomics for peptide syntheses; Pilong Li and Hui-Chun Cheng for help with SH3(2)-PRM affinity measurements; Jonathon Ditlev for critical reading of the manuscript; and Jack Taunton and Julia Okrut (University of California, San Francisco) for communicating unpublished data on the L1/N-WASP/GBD interaction. This work was supported by the Howard Hughes Medical Institute Collaborative Innovation Awards (HCIA) program of the Howard Hughes Medical Institute (S.B., M.K.R.), grants from the NIH (Grant R01-GM56322 to M.K.R.), the Welch Foundation (Grant I–1544 to M.K.R.), the Chilton Foundation (M.K.R.), and the National Science Foundation (Grant MCB 1121867 to R.V.P.). NMR spectroscopy in the Rosen lab is supported by NIH instrumentation grants 1S10RR26461-1 and 1S10OD018027-01.

1. Spector DL (2006) SnapShot: Cellular bodies. *Cell* 127(5):1071.
2. Hyman AA, Simons K (2012) Cell biology. Beyond oil and water–phase transitions in cells. *Science* 337(6098):1047–1049.
3. Brangwynne CP, et al. (2009) Germline P granules are liquid droplets that localize by controlled dissolution/condensation. *Science* 324(5935):1729–1732.
4. Brangwynne CP, Mitchison TJ, Hyman AA (2011) Active liquid-like behavior of nucleoli determines their size and shape in Xenopus laevis oocytes. *Proc Natl Acad Sci USA* 108(11):4334–4339.
5. Wang JT, et al. (2014) Regulation of RNA granule dynamics by phosphorylation of serine-rich, intrinsically disordered proteins in C. elegans. *eLife* 3:e04591.
6. Wippich F, et al. (2013) Dual specificity kinase DYRK3 couples stress granule condensation/dissolution to mTORC1 signaling. *Cell* 152(4):791–805.
7. Zwicker D, Decker M, Jaensch S, Hyman AA, Jülicher F (2014) Centrosomes are autocatalytic droplets of pericentriolar material organized by centrioles. *Proc Natl Acad Sci USA* 111(26):E2636–E2645.
8. Li P, et al. (2012) Phase transitions in the assembly of multivalent signalling proteins. *Nature* 483(7389):336–340.
9. Banjade S, Rosen MK (2014) Phase transitions of multivalent proteins can promote clustering of membrane receptors. *eLife* 3:e04123.
10. Fromm SA, et al. (2014) In vitro reconstitution of a cellular phase-transition process that involves the mRNA decapping machinery. *Angew Chem Int Ed Engl* 53(28):7354–7359.
11. Han TW, et al. (2012) Cell-free formation of RNA granules: Bound RNAs identify features and components of cellular assemblies. *Cell* 149(4):768–779.

12. Kato M, et al. (2012) Cell-free formation of RNA granules: Low complexity sequence domains form dynamic fibers within hydrogels. *Cell* 149(4):753–767.
13. Martino M, Coviello A, Tamburro AM (2000) Synthesis and structural characterization of poly(LGGVG), an elastin-like polypeptide. *Int J Biol Macromol* 27(1):59–64.
14. Mayer BJ (2001) SH3 domains: Complexity in moderation. *J Cell Sci* 114(Pt 7):1253–1263.
15. Nott TJ, et al. (2015) Phase transition of a disordered nuage protein generates environmentally responsive membraneless organelles. *Mol Cell* 57(5):936–947.
16. Ramaswami M, Taylor JP, Parker R (2013) Altered ribostasis: RNA-protein granules in degenerative disorders. *Cell* 154(4):727–736.
17. Gilks N, et al. (2004) Stress granule assembly is mediated by prion-like aggregation of TIA-1. *Mol Biol Cell* 15(12):5383–5398.
18. Jones N, et al. (2006) Nck adaptor proteins link nephrin to the actin cytoskeleton of kidney podocytes. *Nature* 440(7085):818–823.
19. Antoku S, Saksela K, Rivera GM, Mayer BJ (2008) A crucial role in cell spreading for the interaction of Abl PxxP motifs with Crk and Nck adaptors. *J Cell Sci* 121(Pt 18): 3071–3082.
20. Buday L, Wunderlich L, Tamás P (2002) The Nck family of adapter proteins: regulators of actin cytoskeleton. *Cell Signal* 14(9):723–731.
21. Bladt F, et al. (2003) The murine Nck SH2/SH3 adaptors are important for the development of mesoderm-derived embryonic structures and for regulating the cellular actin network. *Mol Cell Biol* 23(13):4586–4597.
22. Cowan CA, Henkemeyer M (2001) The SH2/SH3 adaptor Grb4 transduces B-ephrin reverse signals. *Nature* 413(6852):174–179.
23. Garrity PA, et al. (1996) Drosophila photoreceptor axon guidance and targeting requires the dreadlocks SH2/SH3 adapter protein. *Cell* 85(5):639–650.
24. Rohatgi R, Nollau P, Ho HY, Kirschner MW, Mayer BJ (2001) Nck and phosphatidylinositol 4,5-bisphosphate synergistically activate actin polymerization through the N-WASP-Arp2/3 pathway. *J Biol Chem* 276(28):26448–26452.
25. Ditlev JA, et al. (2012) Stoichiometry of Nck-dependent actin polymerization in living cells. *J Cell Biol* 197(5):643–658.
26. Weisswange I, Newsome TP, Schleich S, Way M (2009) The rate of N-WASP exchange limits the extent of ARP2/3-complex-dependent actin-based motility. *Nature* 458(7234):87–91.
27. Gruenheid S, et al. (2001) Enteropathogenic E. coli Tir binds Nck to initiate actin pedestal formation in host cells. *Nat Cell Biol* 3(9):856–859.
28. Campellone KG, et al. (2004) Clustering of Nck by a 12-residue Tir phosphopeptide is sufficient to trigger localized actin assembly. *J Cell Biol* 164(3):407–416.
29. Eden S, Rohatgi R, Podtelejnikov AV, Mann M, Kirschner MW (2002) Mechanism of regulation of WAVE1-induced actin nucleation by Rac1 and Nck. *Nature* 418(6899): 790–793.
30. Mayer BJ, Eck MJ (1995) SH3 domains. Minding your p's and q's. *Curr Biol* 5(4): 364–367.
31. Ren R, Mayer BJ, Cicchetti P, Baltimore D (1993) Identification of a ten-amino acid proline-rich SH3 binding site. *Science* 259(5098):1157–1161.
32. Takeuchi K, Sun ZY, Park S, Wagner G (2010) Autoinhibitory interaction in the multidomain adaptor protein Nck: Possible roles in improving specificity and functional diversity. *Biochemistry* 49(27):5634–5641.
33. Rivera GM, Briceño CA, Takeshima F, Snapper SB, Mayer BJ (2004) Inducible clustering of membrane-targeted SH3 domains of the adaptor protein Nck triggers localized actin polymerization. *Curr Biol* 14(1):11–22.
34. Gout I, et al. (1993) The GTPase dynamin binds to and is activated by a subset of SH3 domains. *Cell* 75(1):25–36.
35. Musacchio A, Saraste M, Wilmanns M (1994) High-resolution crystal structures of tyrosine kinase SH3 domains complexed with proline-rich peptides. *Nat Struct Biol* 1(8): 546–551.
36. Yu H, et al. (1994) Structural basis for the binding of proline-rich peptides to SH3 domains. *Cell* 76(5):933–945.
37. Padrick SB, et al. (2008) Hierarchical regulation of WASP/WAVE proteins. *Mol Cell* 32(3):426–438.
38. Padrick SB, Doolittle LK, Brautigam CA, King DS, Rosen MK (2011) Arp2/3 complex is bound and activated by two WASP proteins. *Proc Natl Acad Sci USA* 108(33): E472–E479.
39. Doolittle LK, Rosen MK, Padrick SB (2013) Measurement and analysis of in vitro actin polymerization. *Methods Mol Biol* 1046:273–293.
40. Padrick SB, Rosen MK (2010) Physical mechanisms of signal integration by WASP family proteins. *Annu Rev Biochem* 79:707–735.
41. Vitalis A, Pappu RV (2009) ABSINTH: A new continuum solvation model for simulations of polypeptides in aqueous solutions. *J Comput Chem* 30(5):673–699.
42. Mittal A, Lyle N, Harmon TS, Pappu RV (2014) Hamiltonian Switch Metropolis Monte Carlo Simulations for Improved Conformational Sampling of Intrinsically Disordered Regions Tethered to Ordered Domains of Proteins. *J Chem Theory Comput* 10(8): 3550–3562.
43. Flory PJ (1953) *Principles of Polymer Chemistry* (Cornell University Press, Ithaca, NY), 1st Ed.
44. Semenov AN, Rubinstein M (1998) Thermoreversible gelation in solutions of associative polymers. 1. Statics. *Macromolecules* 31(4):1373–1385.
45. Lettau M, Pieper J, Janssen O (2009) Nck adapter proteins: Functional versatility in T cells. *Cell Commun Signal* 7:1.
46. Obenauer JC, Cantley LC, Yaffe MB (2003) Scansite 2.0: Proteome-wide prediction of cell signaling interactions using short sequence motifs. *Nucleic Acids Res* 31(13): 3635–3641.
47. Mayya V, et al. (2009) Quantitative phosphoproteomic analysis of T cell receptor signaling reveals system-wide modulation of protein-protein interactions. *Sci Signal* 2(84):ra46.
48. Dephoure N, et al. (2008) A quantitative atlas of mitotic phosphorylation. *Proc Natl Acad Sci USA* 105(31):10762–10767.
49. Abdul-Manan N, et al. (1999) Structure of Cdc42 in complex with the GTPase-binding domain of the 'Wiskott-Aldrich syndrome' protein. *Nature* 399(6734):379–383.
50. Kim AS, Kakalis LT, Abdul-Manan N, Liu GA, Rosen MK (2000) Autoinhibition and activation mechanisms of the Wiskott-Aldrich syndrome protein. *Nature* 404(6774): 151–158.
51. Okrut J, Prakash S, Wu Q, Kelly MJS, Taunton J (2015) Allosteric N-WASP activation by an inter-SH3 domain linker in Nck. *Proc Natl Acad Sci USA* 112:E6436–E6445.
52. Cheng HC, Skehan BM, Campellone KG, Leong JM, Rosen MK (2008) Structural mechanism of WASP activation by the enterohaemorrhagic E. coli effector EspF(U). *Nature* 454(7207):1009–1013.
53. Keller S, et al. (2012) High-precision isothermal titration calorimetry with automated peak-shape analysis. *Anal Chem* 84(11):5066–5073.
54. Houtman JC, et al. (2007) Studying multisite binary and ternary protein interactions by global analysis of isothermal titration calorimetry data in SEDPHAT: Application to adaptor protein complexes in cell signaling. *Protein Sci* 16(1):30–42.
55. Delaglio F, et al. (1995) NMRPipe: A multidimensional spectral processing system based on UNIX pipes. *J Biomol NMR* 6(3):277–293.
56. Johnson BA, Blevins RA (1994) NMR View: A computer program for the visualization and analysis of NMR data. *J Biomol NMR* 4(5):603–614.
57. Muhandiram DR, Kay LE (1994) Gradient-enhanced triple-resonance three-dimensional NMR experiments with improved sensitivity. *J Magn Reson B* 103(3):203–216.
58. Robert X, Gouet P (2014) Deciphering key features in protein structures with the new ENDscript server. *Nucleic Acids Res* 42(Web Server issue):W320–W324.